Comparative Study on Surface-Mounted Permanent Magnet Motors With Segmented and Connected Core for Brake System

BAIK-KEE SONG[1], **DAE-KEE KIM**[1], **SUNG-IL KIM**[2], (Member, IEEE), **HYEON-JIN PARK**[3], **GEUN-HO LEE**[4], **AND MYUNG-SEOP LIM**[1], (Member, IEEE)

[1]Department of Automotive Engineering, Hanyang University, Seoul 04763, South Korea
[2]Department of Electrical Engineering, Hoseo University, Asan-si 31499, South Korea
[3]Department of Electro-mechanical System Research Team, Electrification System Research and Development Center, Korea Automotive Technology Institute (KATECH), Daegu 43011, South Korea
[4]Department of Automotive Engineering, Kookmin University, Seoul 02707, South Korea

Corresponding author: Myung-Seop Lim (myungseop@hanyang.ac.kr)

ABSTRACT The performance of motors can vary considerably, depending not only on the design but also the manufacturing process. In particular, for motors used in systems wherein vibration and noise are important, the characteristics of the motors change according to the manufacturing method; hence, it is essential to study the effect of the manufacturing process on the characteristics of motors. In this study, motors with a connected core and segmented core are compared and analyzed; particularly, the motors are intended for use in a brake system. The general strengths and weaknesses of each core type are determined, and the electrical and mechanical properties of the motors are analyzed through finite element analysis (FEA). The motors are applied to an integrated brake system that does not employ a vacuum booster, and motors with each type of core are fabricated and tested to verify their characteristics. Finally, the analysis results obtained using FEA and the test results are compared and analyzed to evaluate the validity of this study.

INDEX TERMS Connected core, electromagnetic force, integrated brake system, manufacturing tolerance, mechanical tolerance, noise and vibration, segmented core, torque ripple.

I. INTRODUCTION

Recently, the growing importance of both energy-efficient internal combustion engines and eco-friendly vehicles has led to the replacement of hydraulic and mechanical systems with electrical systems driven by electric motors. The electric power steering system is representative of such systems. Research and development on the use of a motor instead of a hydraulic device to generate pressure in the brake system has been intensively carried out; moreover, this system has been applied to some vehicles. Consequently, the role of the motor in vehicles has become increasingly important to improve fuel efficiency or driving distance on a single charge.

Motor design for automotive applications is a complex task that requires consideration of motor performance and size as well as manufacturing costs and productivity.

The associate editor coordinating the review of this manuscript and approving it for publication was Kan Liu.

However, recent studies on motor design have focused on rotor shape design for increased power, for example, studies on multilayer interior permanent magnet (PM) motors [1]–[3]. As a result, there is little research on actual manufacturing. Most studies concerning manufacturing have also focused on cogging torque analysis. Zhu investigated the effect of additional air gaps, which occur owing to manufacturing tolerances, on the cogging torque in modular stator lamination structures [4]. Gasparin discussed the sensitivity of PM assembly tolerances as well as width and thickness variations [5]. Islam studied the cogging torque by considering stator lamination anisotropies and eccentricities as well as the effect of the aforementioned tolerances on mass production [6]. Kitamura presented an analytical expression of the cogging torque caused by roundness errors of the stator [7].

This paper deals with the electrical and mechanical properties of motors with two types of cores, i.e., segmented and connected cores [8], and the advantages and disadvantages
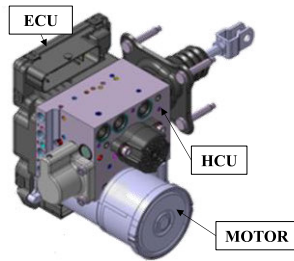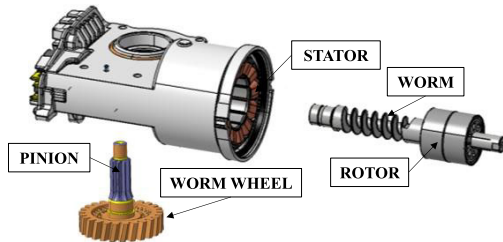
FIGURE 1. Integrated brake system.
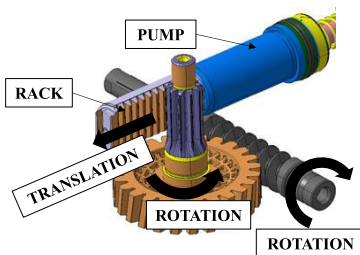

FIGURE 2. Motor component.

FIGURE 3. Rotational motion to translational motion.

TABLE 1. Motor specifications for integrated brake system.

Description	Value
Motor type	SPMSM
Pole / slot	8 / 12
Air gap [mm]	0.7
Max. operation speed [rpm]	6000
Max. torque [Nm]	3

stability control and ABS modules are integrated into a single box consisting of a hydraulic control unit (HCU), an electronic control unit (ECU), and motor assembly, as shown in Fig. 1. The motor assembly consists of a motor, worm, worm wheel, and pinion. The structure is shown in Fig. 2. The motor shaft is integrated with the worm. The worm and worm wheel have a particular gear ratio; hence, the worm wheel rotates depending on the gear ratio when the rotor rotates once. The integrated brake system operates in the following sequence. When the driver steps on the brake pedal, current flows into the motor. Simultaneously, the pedal simulator in the HCU simulates the pedal feeling of the driver, and the signal of the pedal sensor in the brake pedal is transmitted to the ECU. The ECU applies the motor current to generate the appropriate hydraulic pressure corresponding to the pedal input. The motor generates torque, amplifies it through the worm and worm wheel gear connected to the motor shaft, and transmits it to the pinion. The pinion is connected to the rack; the rack is connected to the pump, which ultimately converts the rotational motion of the motor into the translational motion of the pump. Fig. 3 describes the principles of rotational motion and translational motion. Increasing the motor current causes the pump to advance and deliver the brake fluid to the caliper of each wheel to generate the pressure in the four wheels. When the pressure is released, the motor current is reduced, and the pump is moved backward by the hydraulic pressure in the caliper because the pressure on the caliper side is higher than the pressure generated by the motor torque. Thus, the motor always operates when the brake is actuated. The motor specifications for the integrated brake system are listed in Table 1. and the operating steps of the brake system are shown in Fig. 4.

of different manufacturing techniques. The motor is applied to an integrated brake system without a vacuum booster. The motors to which each core is applied are fabricated and tested to verify their performance. The electrical and mechanical characteristics of each core are analyzed numerically and compared with the test results of applying both motors to brake systems. In particular, the noise and vibration source of the brake system to which each core is applied are analyzed through measurement and analysis of results. This paper presents the following: (1) a comparison of the figures and characteristics of segmented and connected cores according to the manufacturing methods; (2) the overall advantages and disadvantages of the segmented and connected cores; (3) analysis of the electrical and mechanical characteristics of segmented and connected cores; and (4) noise, vibration, and harshness evaluation of the brake system in a vehicle equipped with a segmented core and connected cores.

II. PRINCIPLE OF A BRAKE SYSTEM
Conventional brake systems generate pressure from a vacuum pump or vacuum booster using the intake manifold of the engine, and an anti-lock brake system (ABS) module is installed to configure the whole brake system. The brake system introduced in this study is one in which the existing hydraulic booster is replaced with a motor, and the electronic

III. STRUCTURE OF A STATOR CORE
Generally, the stator core generally consists of a one-piece core, segmented core, and connected core [9]. The one-piece core has a limit on the size of the coil winding nozzle, which decreases the fill factor, but it can also reduce the roundness error caused by the manufacturing process. However, owing to the nozzle size, it is subject to design restrictions, such as a slot open. The segmented core can have a high fill factor by combining each divided core after coil winding. However, the roundness may deteriorate depending on the assembly tolerance level. This increases the harmonic components of the radial force which is local electromagnetic force and the harmonic components of tangential forces which increases the torque ripple and cogging torque that cause unwanted vibration and noise components [10], [13]–[19]. Moreover,
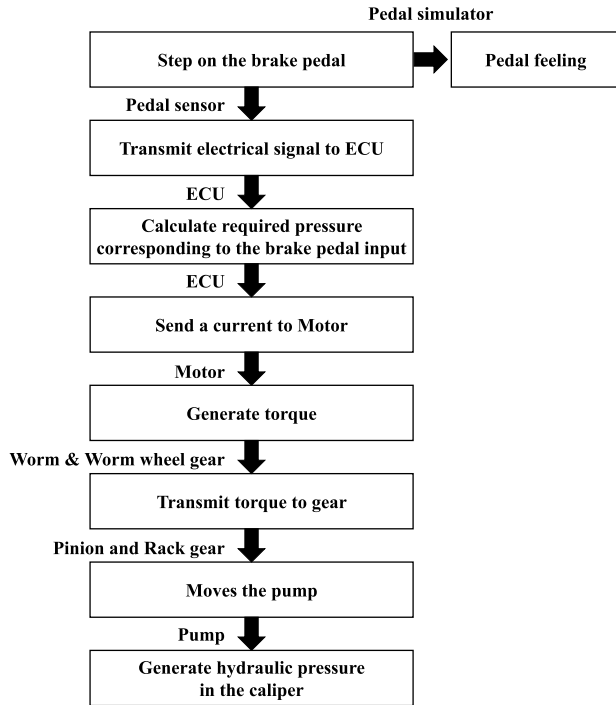
FIGURE 4. Operating sequence of the brake system.

if the number of slots is large, the assembly cost may increase. With regard to the connected core, the fill factor may decrease depending on the nozzle diameter [8]. Furthermore, a long string of lamination pieces is rolled together and connected by welding on one side; therefore, the roundedness of the connected core may deteriorate owing to unwanted tolerances, similar to the case of the segmented core. This could have an adverse effect on the noise and vibration. However, when the coil is connected in series, the number of fusing points due to the bus bar is reduced, and the number of bus bars is reduced compared with that in the segmented core. Therefore, there is room for reducing the overall size and cost of the motor in accordance with the number of bus bars reduced by manufacturing the connected core.

The difference between the segmented core and connected core is shown in Fig. 5. In the connected core, the entire stator core, in the form of a straight line that connects each stator tooth in one electrical steel sheet, was obtained through a pressing process, as shown in Fig. 5(a). After stacking each sheet through interlocking, coil winding is performed with the expanded stator core. The nozzle winds the coil around one tooth, and then it moves to the next tooth corresponding to the same phase to wind the coil around that tooth. After coil winding, the stator core is assembled via banding, the beginning and end of the stator tooth are welded and made into a single stator. In contrast, the segmented core is a type of core obtained by stamping a sheet of stator core tooth through a press process, as shown in Fig. 5(b), and then stacking each sheet by interlocking. After winding the stator coil around each stator tooth, each stator tooth is assembled into a circular shape and made into a single stator via the
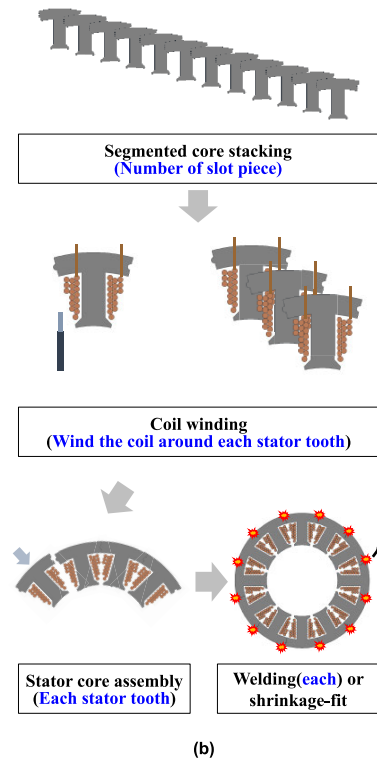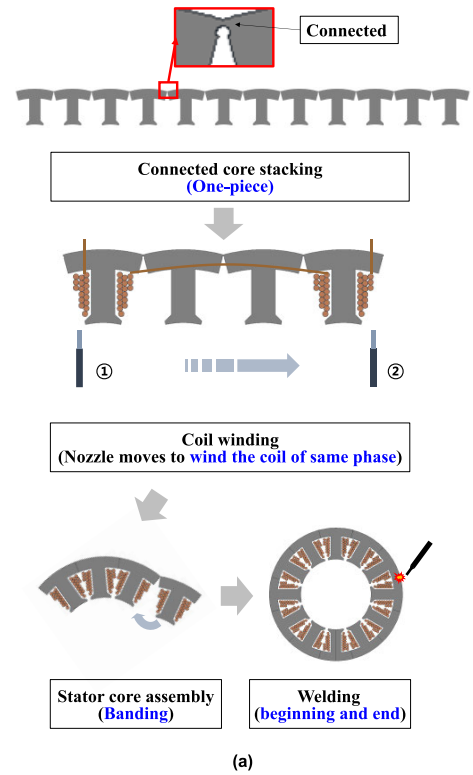

FIGURE 5. Stator core manufacturing process and core shapes (a) Connected core (b) Segmented core.

welding or shrinkage-fitting of the motor housing. As the connected core has an unfolded stator, the nozzle size is not limited by slot open; therefore, the coil can be wound over a certain number of turns compared with the one-piece core.
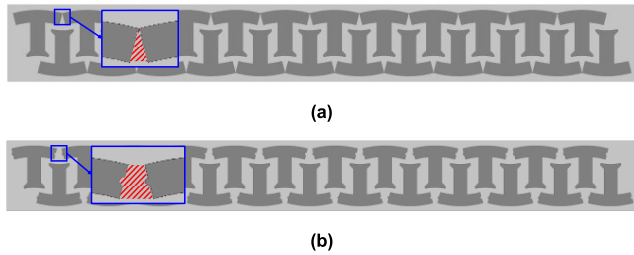
FIGURE 6. Scrap differences between cores (a) Connected core sheet after blanking (b) Segmented core sheet after blanking.

One advantage is that a bus connection is not necessary when winding the coil over one tooth to the next. Another advantage is that the scrap rate of the electrical steel sheet can be reduced, thus reducing the material cost, as shown in Fig. 6. The red regions in Figs. 6(a) and 6(b) illustrate the scrap rate differences between cores. Although the difference in the scrap in Fig. 6 seems very small and there is no significant difference in the cost per unit, the difference in cost is significant in mass production. Administrative expenses can also be reduced because in the case of the connected core, only a piece of the core is manufactured and handled. However, with regard to the segmented core, cores that are as many as the number of slots are manufactured and handled. As a result, in the case of the connected core, conversion costs (e.g., packing, crating, and handling costs) and administrative costs are reduced.

IV. FEA ANALYSIS USING COMMERCIAL TOOLS

In the previous section, the productivity and costs of connected and segmented cores were compared. In this section, the differences in the stator core shape or motor according to the manufacturing method are described. The electrical and mechanical characteristics of each core type are analyzed and compared via finite element analysis (FEA). These include average torque, cogging torque, torque ripple, and displacement of stator by radial electromagnetic force.

A. FEATURE OF CORES

Fig. 7 shows the results of a computed tomography (CT) scan of a motor with a segmented core and connected core. The pictures obtained from the CT scanner show the upper section of the motor. As the motor in this paper is intended for mass production, it is necessary to secure a sufficient insulation distance for the coils between different phases to minimize the defect rate. Therefore, the fill factor of the connected and segmented cores in Fig. 7 is designed considering mass production. The most substantial difference between the two cores can be observed in the joint, as shown by the red circles in Fig. 7(a). To maintain the roundness of the stator or minimize the stress due to core interference, a design tolerance is considered to prevent the interference between the teeth and another one. Thus, a small hole is formed after assembly, and a large gap is observed between the two teeth in the connected core, as shown in Fig. 7(a), unlike in the

segmented core. In contrast, the segmented core has a small and almost uniform air gap between the teeth, as shown in Fig. 7(b). In the following sections, the changes in electrical and mechanical properties according to the manufacturing method are analyzed.
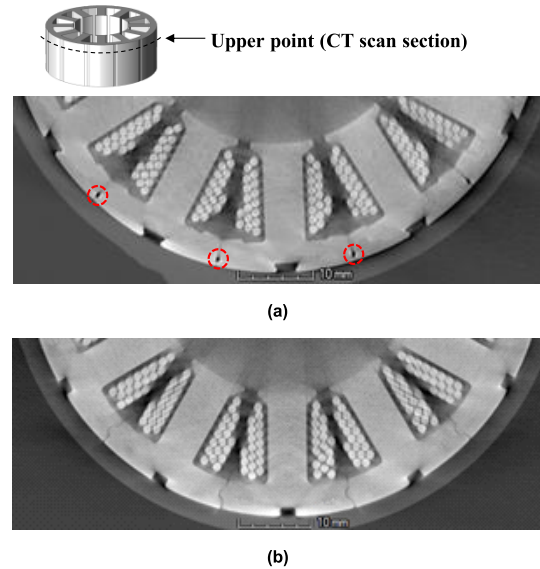

FIGURE 7. Pictures of cores, obtained from a CT scanner: (a) Connected core (b) Segmented core.
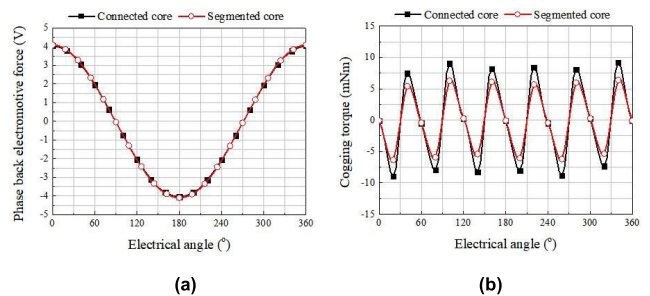

FIGURE 8. No load electrical characteristic of two cores (a) No load back-electromagnetic force (b) cogging torque of connected core and segmented core.

TABLE 2. Electrical properties of motors with different cores in no load condition.

Property	Connected core	Segmented core
Back-emf amplitude [V]	4.06	4.09
THD of back-emf [%]	0.89	0.85
Cogging torque [mNm]	18.1	12.7

B. ELECTRICAL PROPERTIES

The electrical properties of motors with different cores under no-load and load conditions are compared in this section. The no-load electrical properties determined via FEA are shown in Fig. 8 and Table 2. The results were compared when the mechanical tolerances shown in Fig. 9 were equal to zero. The peak and total harmonic distortion (THD) of the back- electromotive force (emf) of the connected and
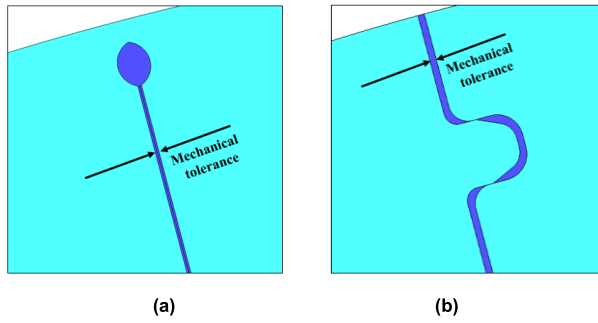
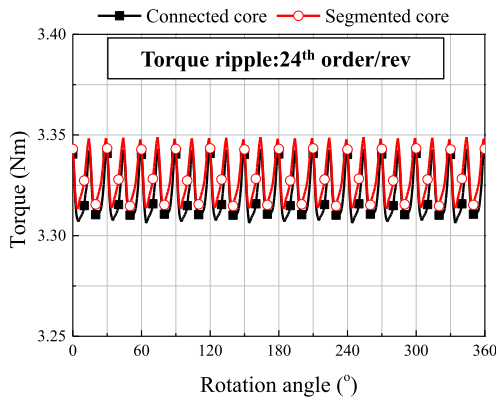**FIGURE 9.** Mechanical tolerance of (a) connected core (b) segmented core.

FIGURE 10. Torque waveforms corresponding to connected and segmented cores.

TABLE 3. Electrical properties of motors with different cores under load.

Property	Connected core	Segmented core
Average torque [Nm]	3.32	3.32
Torque ripple [%]	1.11	1.06

segmented cores are 4.06 V and 4.09 V, and 0.89% and 0.85% respectively. The peak-to-peak cogging torques of the connected and segmented cores are 18.1 mNm and 12.7 mNm, respectively. The electrical properties in the load condition were compared under the same torque of 3.32 Nm, as shown in Fig. 10 and Table 3. The torque ripples of the connected core are 1.11% and 1.06%, respectively. There is no significant difference, but the electrical properties of the connected core tend to be worse than those of the segmented core. In the manufacturing process of connected and segmented cores, air gaps due to mechanical tolerances inevitably occur, as shown in Fig. 9. As the motor mainly operates under the load condition, the torque ripple, which is a load characteristic, was investigated through FEA according to mechanical tolerances. The calculation results are shown in Fig. 11 and Table 4. The torque ripple of the motor increased as the airgap due to mechanical tolerance increased, for a constant torque. When the mechanical tolerances are the same, the torque ripple of the connected core tends to be higher than that of the segmented core. As shown in Fig. 11, the torque ripple of the connected core is more sensitive to tolerance than the segmented core.
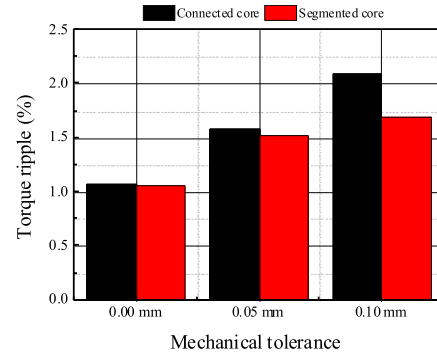
FIGURE 11. Torque ripple of connected and segmented cores according to mechanical tolerance.

TABLE 4. Torque ripple according to mechanical tolerance.

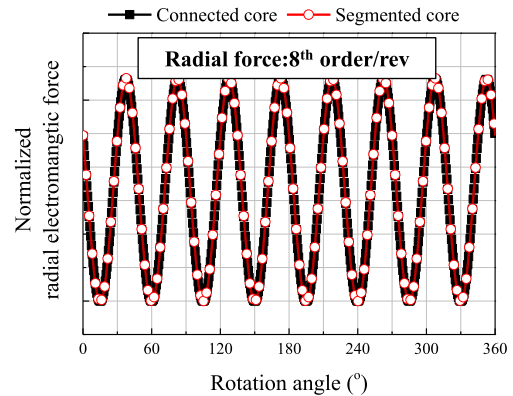| Mechanical tolerance	Torque ripple of connected core	Torque ripple of segmented core
0.00 mm	1.11%	1.06%
0.05 mm	1.58%	1.52%
0.10 mm	2.10%	1.70%

FIGURE 12. Normalized radial electromagnetic force exhibited by connected and segmented cores.

The torque ripple of the gear shaft is transmitted to the entire brake system through the gear system, as shown in Fig. 2 and 3, causing the whole system to vibrate [11]. Because a motor with eight poles is used for the brake system, 24 times of torque fluctuations occur when the rotor rotated once. Then, the 24th-order noise and vibration component of the motor, generated by the torque ripple, can be observed in the system. As mentioned above, the torque ripple generated by the connected core is greater than that of the segmented core, therefore, under similar tolerances, the 24th-order noise and vibration component generated by the torque ripple of the connected core is expected to be greater than that of the segmented core in the system. Fig. 12 shows the normalized radial electromagnetic force generated by the motor with different stator cores. The radial electromagnetic force acts on the teeth of the stator and induces the vibration of the stator. The radial electromagnetic force is calculated at a fixed point in the air gap according to the rotation angle of the rotor; consequently, the main frequency of the radial electromagnetic force is eight times the rotational speed.
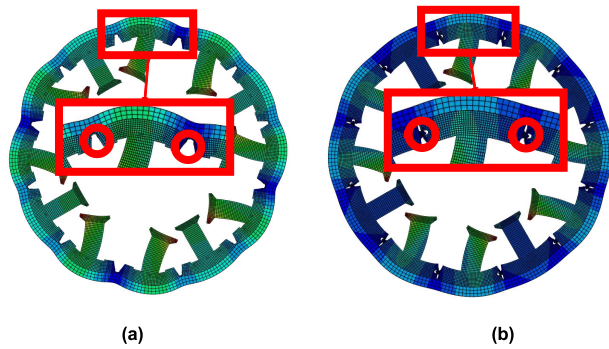
FIGURE 13. Housing-stator core displacement of (a) connected core (b) segmented core.

FIGURE 14. Cycles of displacement in different cores at one node.

TABLE 5. Displacements exhibited by motors with different core types under load.

Mechanical tolerance		Displacement of connected core	Displacement of segmented core
0.00 mm	Avg.	19.67 nm	11.55 nm
	Max.	28.87 nm	17.18 nm
0.05 mm	Avg.	19.90 nm	11.58 nm
	Max.	28.87 nm	17.19 nm

The vibration induced by the radial electromagnetic force can be measured based on the eight-order component. Because the amplitudes of the radial electromagnetic forces exhibited by connected and segmented cores are similar, the vibration at the eighth-order component might be measured in a similar manner. However, the characteristics of the stator core structure also affect the vibration, even under same excitation force. Thus, the mechanical properties of each core should be considered.

C. MECHANICAL PROPERTIES
A comparison of the mechanical properties of motors with different cores is presented in this section. This analysis was conducted using Abaqus, a commercial FEA tool, via an implicit method. In implicit analysis, Newton–Raphson iterations are performed after each increment to enforce the equilibrium between the internal structural forces and externally applied loads. The equilibrium is usually enforced within some specified tolerance. During the Newton–Raphson iterations, the stiffness matrices are updated and reconstructed for each iteration to being done accurately. The same magnetic forces are applied to all nodes at the end of the teeth, and magnetic forces are time-dependent in transient analysis. In analysis condition, the housing and the stator core are bonded to each other. The displacement of each stator core is calculated by applying the radial electromagnetic force to the teeth of the stator, as shown in Fig. 13.

The results are summarized in Table 5. In the table, the "Avg." value is the average amount of displacement around the periphery of the housing, and "Max." is the value at one point where the magnitude of displacement around the entire housing is the largest. The displacement of the segmented core is approximately 40% of the connected core
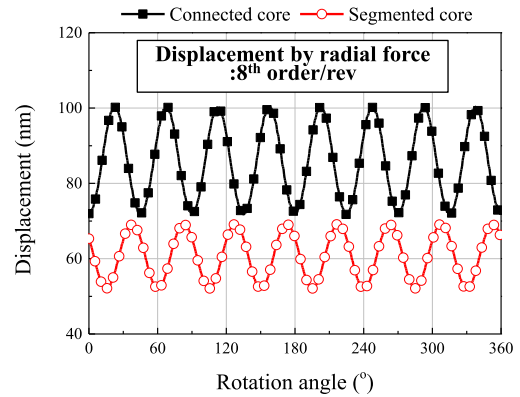
displacement. For the same core type, the mechanical tolerance does not affect the displacement. Fig. 14 shows the displacement of eight cycles per revolution of the rotor at one node point where the maximum displacement fluctuation changes. Although the degree of displacement varied at each node in the housing, the housing was deformed at eight cycles per revolution of the rotor, as shown in Fig. 14. In addition, the fluctuation of the eighth-order component displacement is larger in the connected core than that in the segmented core. The reason for the difference in displacement is the assembly structure between each core. In the case of the connected core, the core ends are connected. In the case of the segmented core, the midpoint of the stator yoke is connected via press fitting; hence, the moment of each tooth is different, as shown in Fig. 13, which affects the overall displacement. This result indicates that the eighth-order noise and vibration component of a motor with a connected core is larger than that of a motor with a segmented core because the amplitude of the applied radial electromagnetic force is similar, as shown in Fig. 12.

V. ANALYSIS BASED ON TEST RESULT
The integrated brake system is located directly on the driver's side panel near the dashboard in the engine room, as shown in Fig. 15. The operating sound produced by the brake system during braking is easily heard by the driver. Therefore, in an integrated brake system, the operating sound is a critical requirement. The operating sound mainly consists of the structure-borne sound from the motor, which excites the system through the worm and worm wheel, and the hydraulic sound generated when a brake fluid passes through the narrow channel of the HCU. However, the hydraulic sound is in the high-frequency region; furthermore, it was excluded from the analysis in this study. As shown in Fig. 15, the brake system was mounted on the vehicle. The operating sound was measured from the driver's seat, whereas the acceleration was measured with acceleration sensors on the HCU and motor, respectively. The noise and vibration were measured in a semi-anechoic room to prevent unwanted reflections.

Table 6 presents the results of the operating sound measurements performed at the driver's seat. In the table, "Apply" indicates the generation of brake pressure, and "Release"
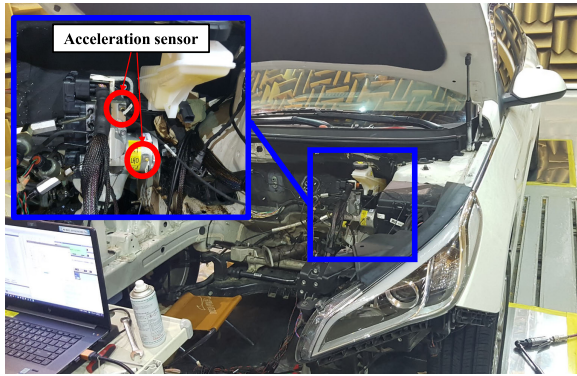
FIGURE 15. Noise and vibration test environment.

TABLE 6. Operating sound level differences between segmented and connected core.

Test Mode			Leq [dB(A)]				
			Segmented core			Connected core	
Pedal rate [mm/s]			#1	#2	#3	#1	#2
60	Slow	Apply	24.8	23.8	23.9	28.1	27.3
		Release	25.0	23.3	22.7	24.1	24.3
90	Medium	Apply	28.0	27.0	27.1	31.5	29.1
		Release	27.7	26.0	25.7	26.6	26.6
120	Fast	Apply	36.3	32.2	30.2	37.0	33.7
		Release	30.9	32.2	29.8	30.7	29.7

indicates the reduction of brake pressure. To improve the reliability of the test, three motors with a segmented core and two motors with a connected core were tested in the same brake system (i.e., same ECU and HCU). Within the same group, the resultant deviation was caused by the mechanical tolerances of each motor that constituted the system. The dominant mechanical tolerances include electric motors as well as worm and worm wheel gear, all of which were added, resulting in the deviation of the overall operating sound level.

The sound level measured at the driver's seat has multiple order components, among which the sound level of the 24th-order component is high, as shown in Fig. 16. The operating sound is believed to have originated from the motor, as the 24th-order noise component is identical to the order of the torque ripple. There also exists a 24th-order vibration component in the HCU and motor, as shown in Fig. 16. The 24th-order vibration component, which was measured in the HCU, is mainly from the motor torque ripple because the motor and HCU were assembled together thorough the gear system [11]. Therefore, the 24th-order vibration component caused by the motor increased the HCU's acceleration and affected the sound level at the driver's seat. The 24th-order vibration component was also measured in the r-direction using the acceleration sensor attached to the motor housing because the torque ripple of the motor excited the HCU connected to the motor shaft; this component is transmitted back to the motor.

The eighth-order component of motor acceleration in Fig. 16 was dominant because the acceleration sensor was
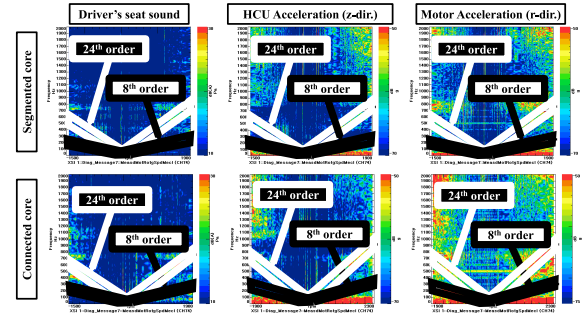

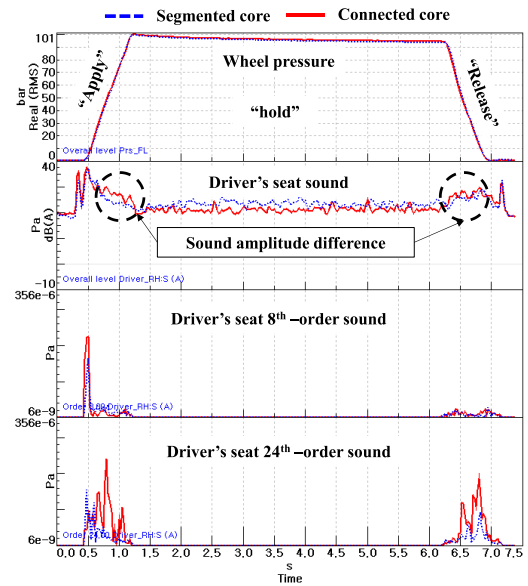**FIGURE 16.** Experimental result corresponding to an automotive brake system.

FIGURE 17. Order-tracking of the operating sound.

located at the top of the stator teeth, which indicates the local force that is radial force [12]. The eighth-order vibration component was predominant in the motor housing, but the eighth-order noise component was not large at the driver's seat because the stator and motor housing was not directly connected to the motor shaft and gear system.

As shown in Table 6, the magnitude of vibration and noise of motors with the connected core increased compared with those of motors with the segmented core. The overall level of the operating sound increased by 2–3 dB(A) in the system with the connected core. Since the fluid noise mainly occurs in the high-frequency range, it is possible to exclude it as the cause of the eighth- and 24th-order noise components. Theoretically, the main noise and vibration components generated by the motor are the 24th-order component, which is the torque ripple arising from the global force, and the eighth-order component generated by the radial force [12]. Thus, as shown in Fig. 17, the sound level was analyzed with regard to the order. The sound level according to the core difference was analyzed by dividing it into the eighth and 24th orders. The noise corresponding to the 24th-order component increased dramatically. This was caused by differences in manufacturing methods for connected and segmented cores
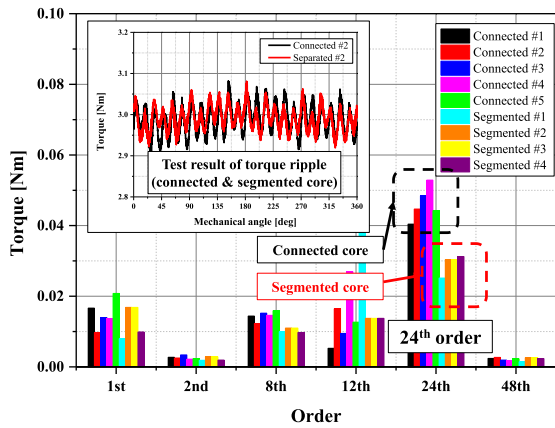
FIGURE 18. Amplitude of 24th order torque ripple under different types of cores.
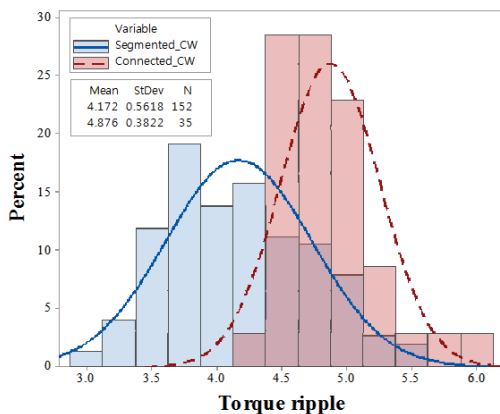

FIGURE 19. Torque ripple histogram for two cores.

when considering a similar level of deviation in the same system. Therefore, it is determined that the difference in the 24th-order noise component measured from the driver's seat is caused by difference between the 24th-order component of the torque ripples of the two types of motors; thus, the 24th-order component of the torque ripple exhibited by the segmented and connected cores was investigated. Fig. 18 shows the magnitude of the torque, determined via discrete Fourier transform (DFT) analysis. The results show that the torque ripple corresponding to the 24th-order component of the connected core increased significantly. To increase the reliability of the result, more samples were investigated to compare the magnitude of the torque ripple between the segmented and connected cores. Since we already know that the main component of the torque ripple is the 24th-order component, in accordance with the DFT computation result shown in Fig. 18, the 24th-order component is expected to increase when the torque ripple of the overall level increases. A total of 152 segmented core samples and 52 connected that the overall magnitude of the connected core torque ripple increased by 0.6% in Fig. 19. Comparison with the previously analyzed results shows that the simulated torque ripple results have the same tendency as the actual test results. Through analysis, the torque ripples at the same torque were compared

that could generate the same pressure on the wheel via the brake. The torque ripple exhibited by the connected core was larger than that of the segmented core. In addition, as the tolerance increased, the increase in the torque ripple of the connected core was greater than that of the segmented core; hence, the increase in the 24th-order vibration and noise component measured in the vehicle originated from the electrical characteristic. The measurement results also confirmed that the 24th-order component of the torque ripple increased in the connected core. The eighth-order component shown in Fig. 17 is attributed to the structural characteristic because the radial forces analyzed via FEA are almost similar, as presented in the previous section. This is because in the analysis results, the eighth-order component of the radial magnetic force is dominant, and the degree of displacement of the connected core, under a similar radial magnetic force, increased by at least two times that of the segmented core.

The test results obtained via FEA, according to core types, are summarized as follows.

· In the brake system with the connected core, the 24th-order sound level is mainly caused by the increased torque ripple (electrical property).

- In the analysis and tests, the torque ripple increased in the connected core.

· The increase in the eighth-order sound level of the brake system with the connected core is mainly attributed to structural differences (mechanical property).

- Although the radial force is similar, the displacement of the motor in the connected core is two times higher in the FEA.

VI. CONCLUSION
In some cases, the connected core has an economic advantage over the segmented core. However, it is still necessary to determine the characteristics according to the manufacturing method of the stator core. In this paper, we presented the mechanical and electrical characteristics of the segmented and connected cores based on FEA; the characteristics were also verified via testing. The torque ripple of the motor was measured and compared. The vibration and noise were also measured for the two types of cores under the system environment. In terms of manufacturing method and cost, the connected core may be more economical; however, from a noise and vibration point of view, the connected core has disadvantages compared with the segmented core. The selection of an appropriate manufacturing method will ensure the desired system performance with regard to noise and vibration.

REFERENCES
[1] L. Zhu, S. Z. Jiang, Z. Q. Zhu, and C. C. Chan, "Analytical modeling of open-circuit air-gap field distributions in multisegment and multilayer interior permanent-magnet machines," *IEEE Trans. Magn.*, vol. 45, no. 8, pp. 3121–3130, Aug. 2009.

[2] D.-K. Lim, K.-P. Yi, D.-K. Woo, H.-K. Yeo, J.-S. Ro, C.-G. Lee, and H.-K. Jung, "Analysis and design of a multi-layered and multi-segmented interior permanent magnet motor by using an analytic method," *IEEE Trans. Magn.*, vol. 50, no. 6, pp. 1–8, Jun. 2014.

[3] S. Zhu, W. Chen, M. Xie, C. Liu, and K. Wang, "Electromagnetic performance comparison of multi-layered interior permanent magnet machines for EV traction applications," *IEEE Trans. Magn.*, vol. 54, no. 11, pp. 1–5, Nov. 2018.

[4] Z. Q. Zhu, Z. Azar, and G. Ombach, "Influence of additional air gaps between stator segments on cogging torque of permanent-magnet machines having modular stators," *IEEE Trans. Magn.*, vol. 48, no. 6, pp. 2049–2055, Jun. 2012.

[5] L. Gasparin, A. Cernigoj, S. Markic, and R. Fiser, "Additional cogging torque components in permanent-magnet motors due to manufacturing imperfections," *IEEE Trans. Magn.*, vol. 45, no. 3, pp. 1210–1213, Mar. 2009.

[6] M. S. Islam, S. Mir, and T. Sebastian, "Issues in reducing the cogging torque of mass-produced permanent-magnet brushless DC motor," *IEEE Trans. Ind. Appl.*, vol. 40, no. 3, pp. 813–820, May 2004.

[7] M. Kitamura, Y. Enomoto, J. Kaneda, and M. Komuro, "Cogging torque due to roundness errors of the inner stator core surface," *IEEE Trans. Magn.*, vol. 39, no. 3, pp. 1622–1625, May 2003.

[8] H. Akita, Y. Nakahara, N. Miyake, and T. Oikawa, "New core structure and manufacturing method for high efficiency of permanent magnet motors," in *Proc. 38th IAS Annu. Meeting Conf. Rec. Ind. Appl. Conf.*, Oct. 2003, pp. 367–372.

[9] W. Tong, "Stator design," in *Mechanical Design of Electric Motors*, 1st ed. Boca Raton, FL, USA: CRC Press, 2017, pp. 219–225.

[10] J.-W. Jung, S.-H. Lee, G.-H. Lee, J.-P. Hong, D.-H. Lee, and K.-N. Kim, "Reduction design of vibration and noise in IPMSM type integrated starter and generator for HEV," *IEEE Trans. Magn.*, vol. 46, no. 6, pp. 2454–2457, Jun. 2010.

[11] D.-Y. Kim, M.-R. Park, J.-H. Sim, and J.-P. Hong, "Advanced method of selecting number of poles and slots for low-frequency vibration reduction of traction motor for elevator," *IEEE/ASME Trans. Mechatronics*, vol. 22, no. 4, pp. 1554–1562, Aug. 2017.

[12] J. F. Gieras, C. Wang, and J. C. Lai, "Magnetic fields and radial forces in polyphase motors fed with sinusoidal currents," in *Noise of Polyphase Electric Motors*. Boca Raton, FL, USA: CRC Press, 2006, p. 21 64.

[13] G. H. Jang and D. K. Lieu, "The effect of magnet geometry on electric motor vibration," *IEEE Trans. Magn.*, vol. 27, no. 6, pp. 5202–5204, Nov. 1991.

[14] I. Hirotsuka, Y. Tsubouchi, and K. Tsuboi, "Effects of slot combination and skew slot on the electromagnetic vibration of a 4 pole capacitor motor under load condition," *J. Electr. Eng. Technol.*, vol. 1, no. 1, pp. 85–91, Mar. 2006.

[15] J.-P. Hong, K.-H. Ha, and J. Lee, "Stator pole and yoke design for vibration reduction of switched reluctance motor," *IEEE Trans. Magn.*, vol. 38, no. 2, pp. 929–932, Mar. 2002.

[16] J.-W. Jung, D.-J. Kim, J.-P. Hong, G.-H. Lee, and S.-M. Jeon, "Experimental verification and effects of step skewed rotor type IPMSM on vibration and noise," *IEEE Trans. Magn.*, vol. 47, no. 10, pp. 3661–3664, Oct. 2011.

[17] T. Sun, J.-M. Kim, G.-H. Lee, J.-P. Hong, and M.-R. Choi, "Effect of pole and slot combination on noise and vibration in permanent magnet synchronous motor," *IEEE Trans. Magn.*, vol. 47, no. 5, pp. 1038–1041, May 2011.

[18] R. Islam and I. Husain, "Analytical model for predicting noise and vibration in permanent-magnet synchronous motors," *IEEE Trans. Ind. Appl.*, vol. 46, no. 6, pp. 2346–2354, Nov. 2010.

[19] D. Fodorean, M. M. Sarrazin, C. S. Martis, J. Anthonis, and H. Van der Auweraer, "Electromagnetic and structural analysis for a surface-mounted PMSM used for light-EV," *IEEE Trans. Ind. Appl.*, vol. 52, no. 4, pp. 2892–2899, Jul. 2016.

DAE-KEE KIM received the bachelor's degree in mechanical engineering from Hanyang University, Seoul, South Korea, in 2014, where he is currently pursuing the Ph.D. degree in automotive engineering. His research interests are the design and optimization of electric machines and analysis of vibration generated by electric machines.

SUNG-IL KIM (Member, IEEE) received the B.S. and M.S. degrees in electrical engineering from Changwon National University, Changwon, South Korea, in 2003 and 2005, respectively, and the Ph.D. degree in automotive engineering from Hanyang University, Seoul, South Korea, in 2011. From 2011 to 2017, he was a Research Staff Member with the Samsung Advanced Institute of Technology (SAIT) and a Senior Engineer with the Compressor and Motor Business Team, Samsung Electronics. He is the holder of five U.S. patents. Since 2017, he has been an Assistant Professor with the Department of Electrical Engineering, Hoseo University, Asan, South Korea. His research interests include multi-physics design optimization of electric machines for robot-driven and automotive applications.

HYEON-JIN PARK received the bachelor's degree in mechanical engineering and the Ph.D. degree in automotive engineering from Hanyang University, Seoul, South Korea, in 2011 and 2020, respectively. From 2014 to 2017, he was a Research Engineer with Keyang, South Korea. Since 2020, he has been a Research Engineer with KATECH. His research interests are electromagnetic field analysis and electric machine design.

GEUN-HO LEE received the B.S. and M.S. degrees in electrical engineering and the Ph.D. degree in automotive engineering from Hanyang University, Seoul, South Korea, in 1992, 1994, and 2010, respectively. From 1994 to 2002, he joined the LG Industrial Research Institute, where he developed inverter system for elevators. Since 2011, he became a Professor of automotive engineering with Kookmin University. His current research interests include the advanced control of electric machines and electric vehicles.

BAIK-KEE SONG received the B.S. degree in mechanical engineering and the M.S. degree in automotive engineering from Hanyang University, in 2009 and 2011, respectively, where he is currently pursuing the Ph.D. degree in automotive engineering. His research interests include electro-magnetic design of motor and motor thermal analysis using equivalent circuit.

MYUNG-SEOP LIM (Member, IEEE) received the bachelor's degree in mechanical engineering and the master's and Ph.D. degrees in automotive engineering from Hanyang University, Seoul, South Korea, in 2012, 2014, and 2017, respectively. From 2017 to 2018, he was a Research Engineer with Hyundai Mobis, Yongin, South Korea. He was an Assistant Professor with Yeungnam University, Daegu, South Korea, in 2018. Since 2019, he has been with Hanyang University, Seoul, South Korea, where he is currently an Assistant Professor. His research interests include electromagnetic field analysis and the design of electric machinery for mechatronics systems, such as automobiles and robotics.

• • •